3

AMBIGUITY FUNCTION

The ambiguity function (AF) represents the time response of a filter matched to a given finite energy signal when the signal is received with a delay τ and a Doppler shift ν relative to the nominal values (zeros) expected by the filter. As explained in Chapter 2, the AF definition followed in this book is

$$|\chi(\tau, \nu)| = \left| \int_{-\infty}^{\infty} u(t) u^*(t + \tau) \exp(j2\pi\nu t)\, dt \right| \tag{3.1}$$

where u is the complex envelope of the signal. A positive ν implies a target moving toward the radar. Positive τ implies a target farther from the radar than the reference ($\tau = 0$) position. The ambiguity function is a major tool for studying and analyzing radar signals. It will serve us extensively in the following chapters, where different signals are described. This chapter presents important properties of the ambiguity function and proves several of them.

3.1 MAIN PROPERTIES OF THE AMBIGUITY FUNCTION

We list the four main properties of the ambiguity function. Proof of the four properties is provided in the next section. The first two properties assume that the energy E of $u(t)$ is normalized to unity.

Radar Signals, By Nadav Levanon and Eli Mozeson
ISBN 0-471-47378-2

Property 1: Maximum at (0,0)

$$|\chi(\tau, \nu)| \leq |\chi(0, 0)| = 1 \tag{3.2}$$

This property says that the ambiguity function can nowhere be higher than at the origin (where it is normalized to unity by normalizing the signal energy).

Property 2: Constant volume

$$\int_{-\infty}^{\infty} \int_{-\infty}^{\infty} |\chi(\tau, \nu)|^2 \, d\tau \, d\nu = 1 \tag{3.3}$$

Property 2 states that the total volume under the normalized ambiguity surface (squared) equals unity, independent of the signal waveform.

Properties 1 and 2 imply that if we attempt to squeeze the ambiguity function to a narrow peak at the origin, that peak cannot exceed a value of 1, and the volume squeezed out of that peak must reappear somewhere else. More restrictions on volume dispersion will be discussed later. The next two properties apply to all signals, normalized or not.

Property 3: Symmetry with respect to the origin

$$|\chi(-\tau, -\nu)| = |\chi(\tau, \nu)| \tag{3.4}$$

Property 3 suggests that it is sufficient to study and plot only two adjacent quadrants of the AF. The remaining two can be deduced from the symmetry property. Our AF plots will usually contain only quadrants 1 and 2 (i.e., positive Doppler values).

Property 4: Linear FM effect
If a given complex envelope $u(t)$ has an ambiguity function $|\chi(\tau, \nu)|$: namely,

$$u(t) \Leftrightarrow |\chi(\tau, \nu)| \tag{3.5}$$

then adding linear frequency modulation (LFM), which is equivalent to a quadratic-phase modulation, implies that

$$u(t) \exp(j\pi k t^2) \Leftrightarrow |\chi(\tau, \nu - k\tau)| \tag{3.6}$$

Property 4 says that adding LFM modulation shears the resulting ambiguity function. The meaning of the shear will be demonstrated following the proof of property 4. This important property is the basis for an important pulse compression technique.

3.2 PROOFS OF THE AF PROPERTIES

Proofs of properties 1 to 4 are presented below. Most of the proofs follow Papoulis (1977).

Property 1: To prove this property, we apply the Schwarz inequality to the AF squared:

$$\begin{aligned} |\chi(\tau, \nu)|^2 &= \left| \int_{-\infty}^{\infty} u(t) u^*(t+\tau) \exp(j2\pi\nu t)\, dt \right|^2 \\ &\le \int_{-\infty}^{\infty} |u(t)|^2\, dt \int_{-\infty}^{\infty} |u^*(t+\tau) \exp(j2\pi\nu t)|^2\, dt \\ &= \int_{-\infty}^{\infty} |u(t)|^2\, dt \int_{-\infty}^{\infty} |u^*(t+\tau)|^2\, dt = E \cdot E = 1 \cdot 1 = 1 \\ &\therefore |\chi(\tau, \nu)|^2 \le 1, \quad \therefore |\chi(\tau, \nu)| \le 1 \end{aligned} \tag{3.7}$$

Equality [i.e., $|\chi(\tau, \nu)|^2 = 1$] will replace the inequality in (3.7) when the functions in the two integrals [second expression in (3.7)] are conjugates of each other: namely, when

$$u(t) = [u^*(t+\tau) \exp(j2\pi\nu t)]^* = u(t+\tau) \exp(-j2\pi\nu t) \tag{3.8}$$

which obviously happens when $\tau = 0$, $\nu = 0$. Thus, we can conclude that

$$|\chi(\tau, \nu)| \le |\chi(0, 0)| = 1 \tag{3.9}$$

Property 2: To prove this property, we rewrite $\chi(\tau, \nu)$, replacing ν with $-f$:

$$\chi(\tau, -f) = \int_{-\infty}^{\infty} [u(t) u^*(t+\tau)] \exp(-j2\pi f t)\, dt \tag{3.10}$$

which is recognized as the Fourier transform

$$\chi(\tau, -f) = F[\beta(\tau, t)] \tag{3.11}$$

of the function

$$\beta(\tau, t) = u(t) u^*(t+\tau) \tag{3.12}$$

The energy in the time domain is equal to the energy in the frequency domain (Parseval's theorem):

$$\int_{-\infty}^{\infty} |\beta(\tau, t)|^2\, dt = \int_{-\infty}^{\infty} |\chi(\tau, -f)|^2\, df = \int_{-\infty}^{\infty} |\chi(\tau, \nu)|^2\, d\nu \tag{3.13}$$

Integrating both sides with respect to τ yields the volume V under the ambiguity function squared

$$\int_{-\infty}^{\infty}\int_{-\infty}^{\infty}|\beta(\tau,t)|^2\,dt\,d\tau=\int_{-\infty}^{\infty}\int_{-\infty}^{\infty}|\chi(\tau,-f)|^2\,df\,d\tau$$
$$=\int_{-\infty}^{\infty}\int_{-\infty}^{\infty}|\chi(\tau,\nu)|^2\,d\nu\,d\tau=V \tag{3.14}$$

We will now evaluate the integral on the left-hand side, starting with a change of variables:

$$t=t_1,\qquad t+\tau=t_2 \tag{3.15}$$

Using (3.12) and (3.15) in (3.14) yields

$$\int_{-\infty}^{\infty}\int_{-\infty}^{\infty}|u(t)u^*(t+\tau)|^2\,dt\,d\tau=\int_{-\infty}^{\infty}\int_{-\infty}^{\infty}|u(t_1)u^*(t_2)|^2|\mathbf{J}(t_1,t_2)|dt_1\,dt_2=V \tag{3.16}$$

where the Jacobian is given by

$$\mathbf{J}(t_1,t_2)=\begin{vmatrix}\dfrac{\partial t_1}{\partial t} & \dfrac{\partial t_1}{\partial \tau}\\[2ex] \dfrac{\partial t_2}{\partial t} & \dfrac{\partial t_2}{\partial \tau}\end{vmatrix}=\begin{vmatrix}1 & 0\\ 1 & 1\end{vmatrix}=1 \tag{3.17}$$

Using (3.17) in (3.16), we get

$$V=\int_{-\infty}^{\infty}\int_{-\infty}^{\infty}|u(t_1)u^*(t_2)|^2|1|dt_1\,dt_2$$
$$=\int_{-\infty}^{\infty}|u(t_1)|^2\,dt_1\int_{-\infty}^{\infty}|u^*(t_2)|^2\,dt_2=E\cdot E=1\cdot 1=1 \tag{3.18}$$

Property 3: To prove this property, we set $-\tau$ and $-\nu$ in the equation for $|\chi(\tau,\nu)|$:

$$\chi(-\tau,-\nu)=\int_{-\infty}^{\infty}u(t)u^*(t-\tau)\exp(-j2\pi\nu t)\,dt \tag{3.19}$$

and make one change of variable, $t_1=t-\tau$, which yields

$$\chi(-\tau,-\nu)=\int_{-\infty}^{\infty}u(t_1+\tau)u^*(t_1)\exp[-j2\pi\nu(t_1+\tau)]\,dt_1$$
$$=\exp(-j2\pi\nu\tau)\int_{-\infty}^{\infty}u(t_1+\tau)u^*(t_1)\exp(-j2\pi\nu t_1)\,dt_1 \tag{3.20}$$
$$=\exp(-j2\pi\nu\tau)\int_{-\infty}^{\infty}u(t+\tau)u^*(t)\exp(-j2\pi\nu t)\,dt$$

Because integration is a linear operation, the integral of a conjugate is equal to the conjugate of the integral; hence,

$$\begin{aligned}\chi(-\tau, -\nu) &= \exp(-j2\pi\nu\tau)\left[\int_{-\infty}^{\infty} u^*(t+\tau)u(t)\exp(j2\pi\nu t)\,dt\right]^* \\ &= \exp(-j2\pi\nu\tau)\chi^*(\tau, \nu) \end{aligned} \tag{3.21}$$

Taking the absolute value yields property 3,

$$|\chi(-\tau, -\nu)| = |\chi(\tau, \nu)| \tag{3.22}$$

Property 4: To prove this property, we define a new complex envelope, in which quadratic phase was added to the original envelope $u(t)$:

$$u_1(t) = u(t)\exp(j\pi k t^2) \tag{3.23}$$

The ambiguity function of $u_1(t)$,

$$u_1(t) \Leftrightarrow |\chi_1(\tau, \nu)| \tag{3.24}$$

is what we look for. This new ambiguity function (without the absolute value) is

$$\begin{aligned}\chi_1(\tau, \nu) &= \int_{-\infty}^{\infty} u_1(t)u_1^*(t+\tau)\exp(j2\pi\nu t)\,dt \\ &= \int_{-\infty}^{\infty} u(t)\exp(j\pi k t^2)u^*(t+\tau)\exp[-j\pi k(t+\tau)^2]\exp(j2\pi\nu t)\,dt \\ &= \exp(-j\pi k\tau^2)\int_{-\infty}^{\infty} u(t)u^*(t+\tau)\exp[j2\pi(\nu - k\tau)t]\,dt \\ &= \exp(-j\pi k\tau^2)\chi(\tau, \nu - k\tau) \end{aligned} \tag{3.25}$$

Taking the absolute value, we get property 4:

$$|\chi_1(\tau, \nu)| = |\chi(\tau, \nu - k\tau)| \tag{3.26}$$

3.3 INTERPRETATION OF PROPERTY 4

Before proceeding to other issues concerning the ambiguity function, it may be worthwhile to interpret property 4, the LFM effect. We explain the shearing caused by the LFM effect with the help of Fig. 3.1. Let the horizontal ellipsoid $|\chi(\tau, \nu)| = c$ be the contour of the original ambiguity function having a specific value c. The contour intersects the negative Doppler axis at point A with the coordinates ($\tau = 0$, $\nu = \nu_A$), and it intersects the positive delay axis at point B

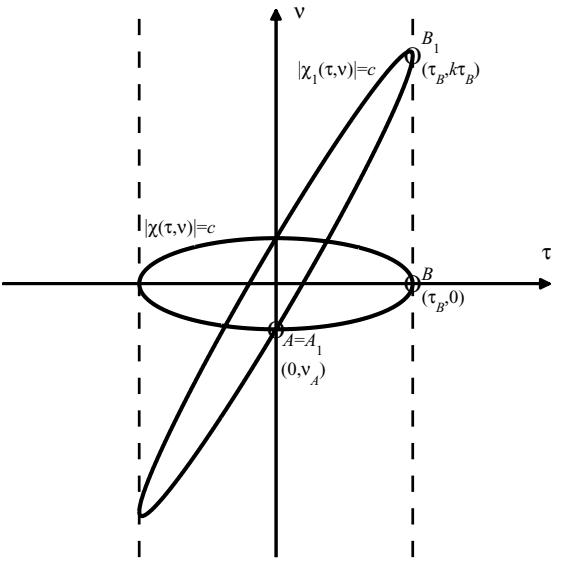

FIGURE 3.1 Linear-FM shearing effect on the ambiguity function.

with the coordinates ($\tau = \tau_B$, $\nu = 0$). The corresponding points A_1 and B_1, of $|\chi_1(\tau, \nu)| = c$, have the same delay coordinates, respectively ($\tau_{A1} = 0$, $\tau_{B1} = \tau_B$). We use (3.26) to find their respective Doppler coordinates, ν_{A1} and ν_{B1}.

Because the delay coordinate of the original intersection of A is zero, we get for A_1

$$c = |\chi_1[0, (\nu_A - k \cdot 0)]| = |\chi_1(0, \nu_A)| \tag{3.27}$$

implying that the Doppler coordinate of A_1 is identical to the Doppler coordinate of A.

Next we ask where the contour $|\chi_1(\tau, \nu)| = c$ meets the delay τ_B; or what is ν_{B1} so that $|\chi_1(\tau_B, \nu_{B1})| = c$? Using (3.26), we get

$$|\chi_1(\tau_B, \nu_{B_1})| = |\chi(\tau_B, \nu_{B_1} - k\tau_B)| = c \tag{3.28}$$

However, in Fig. 3.1 we note that $|\chi(\tau_B, 0)| = c$, which implies that $\nu_{B1} - k\tau_B = 0$, or

$$\nu_{B_1} = k\tau_B \tag{3.29}$$

We thus found that point B at the coordinates ($\tau = \tau_B$, $\nu = 0$), whose delay coordinate is the largest delay through which the contour $|\chi(\tau, \nu)| = c$ passes, was moved, by adding LFM, to point B_1 at the coordinates ($\tau = \tau_B$, $\nu = k\tau_B$). Other points of the contour $|\chi(\tau, \nu)| = c$, at delays $0 < \tau < \tau_B$, were moved in a similar way, thus resulting in the sheared contour $|\chi_1(\tau, \nu)| = c$, also shown

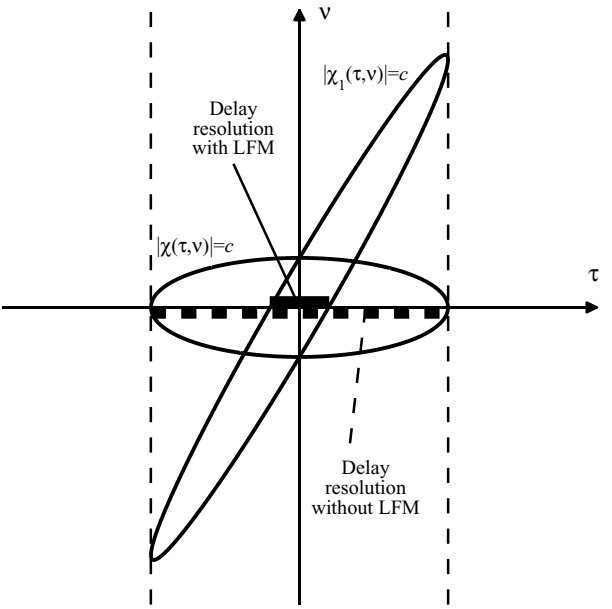

FIGURE 3.2 Improved delay resolution by linear-FM shearing.

in Fig. 3.1. The shearing property of linear FM, which we just studied, reduces (improves) the delay resolution, as pointed out in Fig. 3.2.

Finally, note that for the definition of the ambiguity function used here, the shape of the LFM ridge passing from the third quadrant to the first quadrant of the delay–Doppler space is typical for positive LFM slope ($k > 0$). This implies that for positive LFM slope signal a positive error in estimating target range (the target is assumed to be farther than it really is) will translate to lower closing velocity (negative Doppler).

3.4 CUTS THROUGH THE AMBIGUITY FUNCTION

Some insight into the two-dimensional ambiguity function (AF) can be obtained from its one-dimensional cuts. Consider first the cut along the delay axis. Setting $\nu = 0$ in (3.1) gives

$$|\chi(\tau, 0)| = \left| \int_{-\infty}^{\infty} u(t)u^*(t+\tau)\,dt \right| = |R(\tau)| \tag{3.30}$$

where $R(\tau)$ is the autocorrelation function (ACF) of $u(t)$. We got that the zero-Doppler cut of the AF, known as the *range window* for a matched-filter receiver,

is the ACF. On the other hand, the ACF equals the inverse Fourier transform of the power spectral density. Thus, we get the relationship

$$\text{range window} \;\Leftrightarrow\; \text{autocorrelation} \;\Leftrightarrow \mathbf{F}^{-1}\{\text{power spectrum}\}$$

This relationship reiterates the importance of LFM. Adding linear frequency modulation broadens the power spectrum, hence narrows the range window, as shown in Fig. 3.3.

The second interesting cut is along the Doppler frequency axis. Setting $\tau = 0$ in (3.1) results in

$$|\chi(0, \nu)| = \left| \int_{-\infty}^{\infty} |u(t)|^2 \exp(j2\pi\nu t)\, dt \right| \tag{3.31}$$

Equation (3.31) says that the zero-delay cut is the Fourier transform of the *magnitude* squared of the complex envelope $u(t)$. In other words, this cut is indifferent to any phase or frequency modulation in $u(t)$; it is a function only of the amplitude.

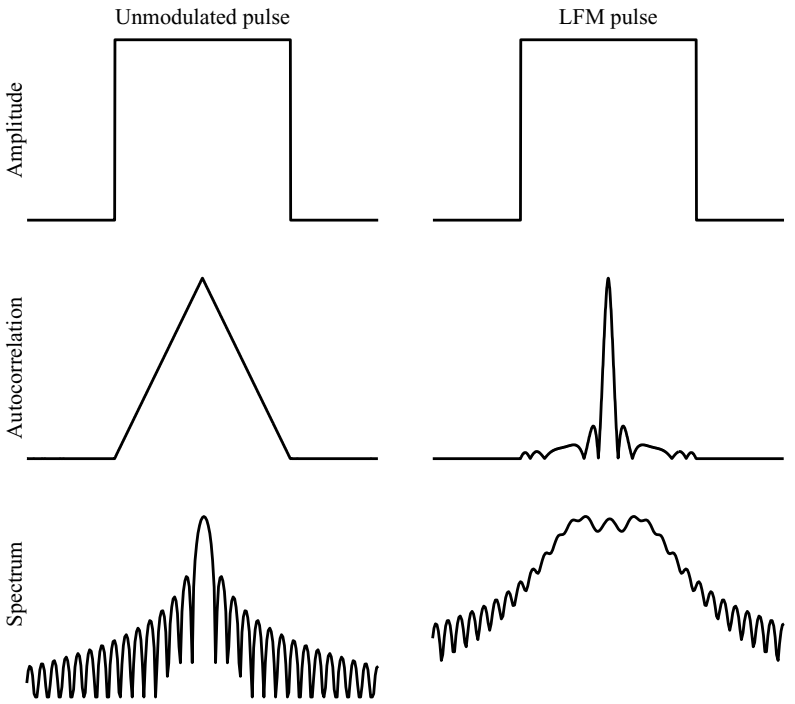

FIGURE 3.3 Comparison between unmodulated pulse and linear-FM pulse.

3.5 ADDITIONAL VOLUME DISTRIBUTION RELATIONSHIPS

The volume distribution of the ambiguity function (squared) in range and in Doppler is constrained by two more refined relationships (Rihaczek, 1969):

$$\int_{-\infty}^{\infty} |\chi(\tau, \nu)|^2 \, d\tau = \int_{-\infty}^{\infty} |\chi(\tau, 0)|^2 \exp(j2\pi\nu\tau) \, d\tau \tag{3.32}$$

$$\int_{-\infty}^{\infty} |\chi(\tau, \nu)|^2 \, d\nu = \int_{-\infty}^{\infty} |\chi(0, \nu)|^2 \exp(j2\pi\nu\tau) \, d\nu \tag{3.33}$$

These two transform relations tell us that if the central peak is squeezed along the delay axis, the volume must spread out in the Doppler domain, and when it is squeezed along the Doppler axis, the volume must spread in delay. Thus, close target separability in one parameter is gained at the expense of spreading volume over a large interval of the other parameter.

3.6 PERIODIC AMBIGUITY FUNCTION

Like the matched filter on which it is based, the ambiguity function is defined for finite-duration signals. However, there are several types of signals that are periodically continuous. Two prominent examples are the periodic continuous-wave (CW) radar signal and a coherent train of *identical* pulses. In both cases, the receiver is usually "matched" to a finite number of periods or pulses, smaller than the number of periods or pulses transmitted. An example of a typical coherent pulse train is shown in Fig. 3.4.

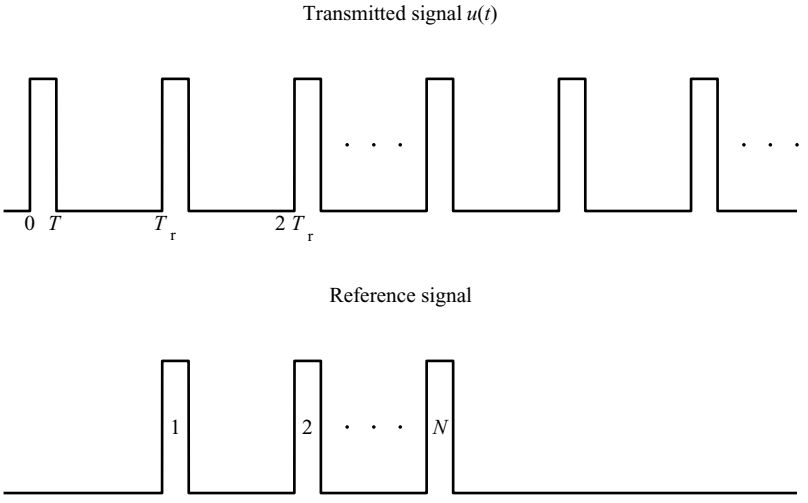

FIGURE 3.4 Processing a coherent pulse train.

To handle this type of signal and processor we define the *periodic ambiguity function* (PAF) and study some of its properties (Freedman and Levanon, 1994; Getz and Levanon, 1995). As shown in Fig. 3.4, a coherent pulse train will help us demonstrate the PAF. We must first explain what the word *coherent* implies. When we introduced the complex envelope of a finite-duration signal (e.g., a pulse), we assumed that the carrier frequency is known. Now, when we consider a train of separated pulses, we need to extend the assumption. We need to assume that the carrier frequency remains the same for all the pulses and that we also know the initial phase of each pulse. A simple variation is to consider the pulses as an interrupted CW signal. In that case the reference signal, constructed from N pulses, can be described as

$$s(t) = \mathrm{Re}[u_N(t)\exp(j2\pi f_c t)] \tag{3.34}$$

and its complex envelope as

$$u_N(t) = \frac{1}{\sqrt{N}}\sum_{n=1}^{N} u_n[t-(n-1)T_r] \tag{3.35}$$

We will usually assume that the pulses are identical: namely, $u_n(t) = u_1(t)$. The complex envelope of the signal received (at zero relative delay and zero Doppler), not limited to N pulses, will be described as an infinite signal:

$$u(t) = \sum_{n=-\infty}^{\infty} u_1[t-(n-1)T_r] \tag{3.36}$$

Doppler-induced phase shifts of the signal received will be handled by the ambiguity function. Other than those phase shifts, (3.36) assumes that the target return exhibits constant phase during the dwell. We now return to Fig. 3.4, where the matched receiver performs a correlation between a received train $u(t)$ of many ($>N$) identical pulses and a reference train $u_N(t)$ of exactly N identical (and same) pulses. The normalized response of this processor, in the presence of Doppler shift, is given by the periodic ambiguity function

$$|\chi_{NT}(\tau,\nu)| = \left|\frac{1}{NT_r}\int_0^{NT_r} u(t)u^*(t+\tau)\exp(j2\pi\nu t)\,dt\right| \tag{3.37}$$

Of special interest is the single-pulse reference signal, which yields

$$|\chi_T(\tau,\nu)| = \left|\frac{1}{T_r}\int_0^{T_r} u(t)u^*(t+\tau)\exp(j2\pi\nu t)\,dt\right| \tag{3.38}$$

Note that as for the aperiodic ambiguity function, a different version of the periodic ambiguity function also exists. In Box 3A some other versions are described and compared to the definition used here.

BOX 3A: Variants of the Periodic Ambiguity Function

The single-period periodic ambiguity function of a signal with complex envelope $u(t)$ was defined in (3.38). The definition in (3.38) represents the straightforward implementation of a filter matched to a signal $u(t)$ delayed by τ and Doppler shifted by ν. Positive values of ν (positive Doppler) represent closing targets, while positive values of τ imply a target farther from the radar than the reference ($\tau = 0$). This definition is not unique. Alternative definitions can be adopted (Freedman and Levanon, 1994). Such definitions are

$$^{1}|\chi_T(\tau, \nu)| = \left| \frac{1}{T_r} \int_0^{T_r} u\left(t - \frac{\tau}{2}\right) u^*\left(t + \frac{\tau}{2}\right) \exp(j2\pi\nu t)\, dt \right| \quad \text{(3A.1)}$$

or

$$^{2}|\chi_T(\tau, \nu)| = \left| \frac{1}{T_r} \int_{-T_r/2}^{T_r/2} u(t)u^*(t + \tau) \exp(j2\pi\nu t)\, dt \right| \quad \text{(3A.2)}$$

These definitions represent an off-line noncasual implementation. For all three definitions the multiperiod ambiguity function relation to the single-period ambiguity function defined in (3.39) holds. Still these definitions are not equivalent, as described below.

Since the signal is periodic with period T_r, the PAF is also periodic in the delay axis direction. The period is T_r for the definitions given in (3.38) or (3A.2). The period of the PAF defined in (3A.1), on the other hand, is $2T_r$.

$$|\chi_T(\tau + nT_r, \nu)| = |\chi_T(\tau, \nu)| \quad \text{(3A.3}a\text{)}$$

$$^{2}|\chi_T(\tau + nT_r, \nu)| = {}^{2}|\chi_T(\tau, \nu)| \quad \text{(3A.3}b\text{)}$$

$$^{1}|\chi_T(\tau + 2nT_r, \nu)| = {}^{1}|\chi_T(\tau, \nu)| \quad \text{(3A.3}c\text{)}$$

Furthermore, the PAF magnitude symmetry with respect to the origin property holds only for the definition given in (3A.1). The other definitions of the PAF, given in (3.37) and (3A.2), are magnitude symmetric with respect to the origin only for $\nu = k/NT_r$ and $\tau = NT$, with k an integer and N the number of periods used.

As in the nonperiodic ambiguity function, there is a constraint on the volume under ambiguity function magnitude. For all three definitions of the periodic ambiguity function described here the volume within a strip of width T_r on the delay axis is equal to 1. For a larger filter length this volume is reduced according to the period-to-filter length ratio (N). The unlimited reduction of the volume as N increases is the result of the unlimited improvement of the Doppler resolution.

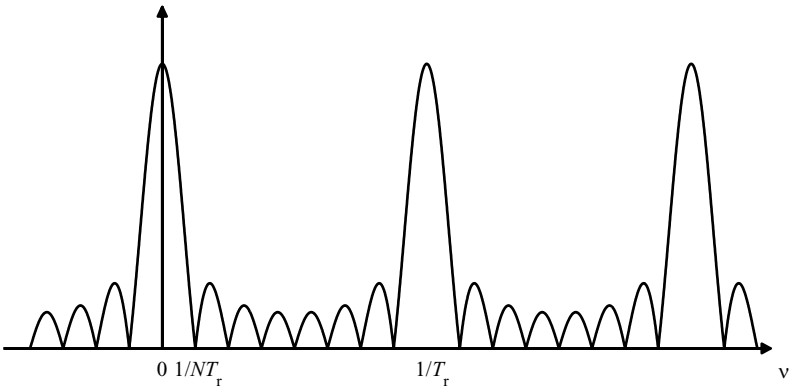

FIGURE 3.5 Function $|(\sin N\pi\nu T_r)/(N \sin \pi\nu T_r)|(N = 8)$.

It can be shown (Freedman and Levanon, 1994; Getz and Levanon, 1995) that a very simple and important relationship exists between equations (3.37) and (3.38):

$$|\chi_{NT}(\tau, \nu)| = |\chi_T(\tau, \nu)| \left| \frac{\sin N\pi\nu T_r}{N \sin \pi\nu T_r} \right| \tag{3.39}$$

Equation (3.39) suggests that it is sufficient to calculate the single-period PAF (3.38) and then multiply it by the function $|(\sin N\pi\nu T_r)/(N \sin \pi\nu T_r)|$ to get the N-period PAF. The multiplying function is a function of the Doppler shift only. Its version for $N = 8$ is plotted in Fig. 3.5.

Figure 3.5 demonstrates the main reason for using a coherent train of N pulses with a repetition interval T_r. Note that the Doppler resolution improves dramatically and becomes $1/NT_r$: namely, the inverse of the coherently processed time duration, and it is practically independent of the original pulse waveform. The penalty is recurrent lobes at Doppler intervals of $1/T_r$: namely, the inverse of the pulse repetition interval. Because the function plotted in Fig. 3.5 multiplies an ambiguity function, which is two-dimensional, it may help to point out that what multiplies the ambiguity function is an extension of Fig. 3.5 to all delays, as demonstrated in Fig. 3.6.

An interesting observation regarding the PAF states that for delays shorter than the pulse duration, $|\tau| \leq T$, the ambiguity function $|\chi(\tau, \nu)|$ is equal to the periodic ambiguity function $|\chi_{NT}(\tau, \nu)|$. This result makes it easier to calculate and plot the partial ambiguity function (for $|\tau| \leq T$) of a signal constructed from N identical pulses. The statement above does not hold for continuous-wave signals nor for pulse trains in which $T_r < 2T$. Coherent pulse trains were introduced here to serve as an example of the need and use of the periodic ambiguity function. The subject of coherent pulse trains will be expanded with much more detail in later chapters.

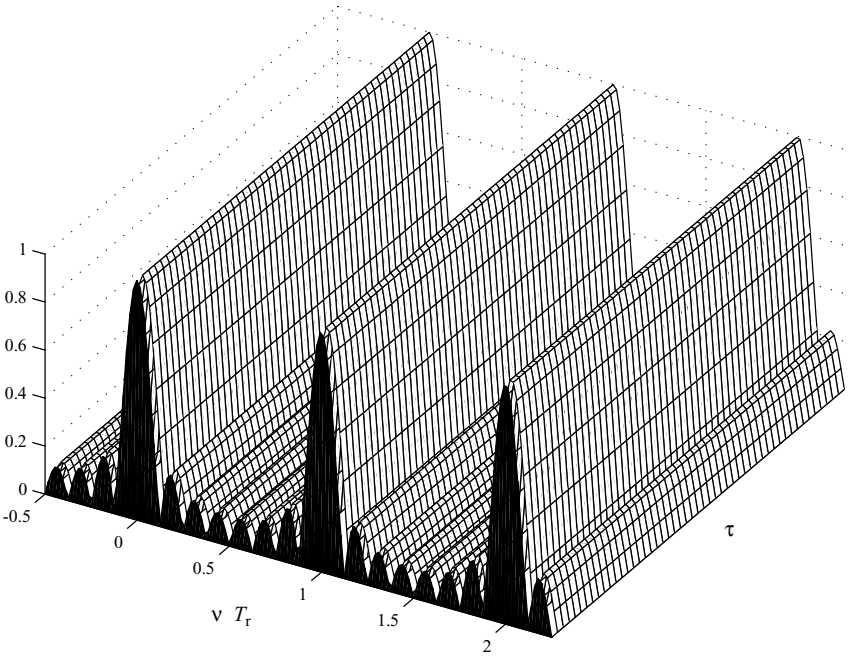

FIGURE 3.6 Extension of $|(\sin N\pi\nu T_r)/(N \sin \pi\nu T_r)|$ to all delays ($N = 8$).

3.7 DISCUSSION

Many types of signals are used for various radar applications and systems. Modern pulse radars generally use pulse compression waveforms (i.e., expanded pulses with larger time–bandwidth products). These kinds of waveforms are applied to obtain high pulse energy (with no increase in peak power) and large pulse bandwidth and, consequently, high range resolution without sacrificing maximum range, which is related to the pulse energy.

Unfortunately, no analytic method exists for calculating a signal given its ambiguity function (*inverse ambiguity transform*); thus the design of a radar signal with desirable characteristics of the ambiguity function is based primarily on the radar designer's prior knowledge of radar waveforms and his or her expertise in such designs. In the following chapters we acquire this knowledge. In Chapter 4 we develop the AF of several basic radar signals. The specific examples will contribute further understanding of the ambiguity function, its properties, and its significance to radar.

The ambiguity function of some of the radar signals to be discussed can be derived analytically. However, many signals are too complicated, and only numerical calculation of their AF is feasible. The most practical means for displaying the numerical result is a three-dimensional plot. The appendix that follows contains a MATLAB program for plotting ambiguity functions (Mozeson and Levanon, 2002).

APPENDIX 3A: MATLAB CODE FOR PLOTTING AMBIGUITY FUNCTIONS

A MATLAB code capable of plotting the ambiguity function $|\chi(\tau, \nu)|$ of many different radar signals is presented. The program makes use of MATLAB's sparse matrix operations, and avoids loops. The code makes it possible to input many different signals and provides control over many plot parameters. The program allows oversampling of the signal with much finer resolution than needed for calculating the delayed signal. This makes it possible to compute a diluted picture (fewer delay–Doppler grid points) of the ambiguity function with low computational effort while sampling the signal with a sufficiently large sampling rate.

Because of the symmetry of the AF with respect to the origin, the code plots only two of the four quadrants. This provides an opportunity to display the zero-Doppler cut of the AF, which is the magnitude of the autocorrelation function. The program also produces a second figure with subplots of three characteristics of the signal: amplitude, phase, and frequency.

Comment on the choice of r: Since the signal is described by a vector, with a well-defined length (number of elements, referred to as M), it is often necessary to increase the number of samples (repeats) during each of these elements (bits), in order to meet the Nyquist criterion. This is the function of r.

For a Costas signal with M elements, the signal bandwidth is approximately M/t_b. Therefore, the sampling interval should be

$$t_s < \frac{t_b}{2M}$$

Hence,

$$\frac{t_b}{t_s} = r > 2M$$

For a phase-coded signal, the main spectral lobe ends at $f = 1/t_b$. However, the spectral sidelobes extend much farther at a rate of approximately 6 dB/octave. A typical spectral skirt crosses the -30 dB level at $f = 10/t_b$. Hence, choosing $r = 2$ is the minimum setting, but using $r > 10$ is recommended.

Note: When a continuation ellipsis (. . .) appears within a single quote, such as a string, it indicates that the string and what follows it (up to a continuation ellipsis that is not within a string) must be completed in the line on which it was started.

The Code

```
% The matlab code plots the ambiguity function of a signal u_basic (row vector)
% The m-file returns a plot of quadrants 1 and 2 of the ambiguity function
%   of a signal
% The ambiguity function is defined as:
%
```

```
% a(t,f) = abs ( sum i( u(k)*u'(i+t)*exp(j*2*pi*f*i) ) )
%
% The user is prompted for the signal data:
% u_basic is a row complex vector representing amplitude and phase
% f_basic is a corresponding frequency coding sequence
%
% The duration of each element is tb (total duration of the signal is
%   tb*(m_basic-1))
%
% F is the maximal Doppler shift
% T is the maximal Delay
% K is the number of positive Doppler shifts (grid points)
% N is the number of delay shifts on each side (for a total of 2N+1 points)
% The code allows r samples within each bit
%
% Written by Eli Mozeson and Nadav Levanon, Dept. of EE-Systems, Tel Aviv
%   University

clear all

% prompts for signal data

u_basic=input(' Signal elements (row complex vector, each element last tb ...
  sec) = ? ');
m_basic=length(u_basic);

fcode=input(' Allow frequency coding (yes=1, no=0) = ? ');
if fcode==1
    f_basic=input(' Frequency coding in units of 1/tb (row vector of same ...
      length) = ? ');
end

F=input(' Maximal Doppler shift for ambiguity plot [in units of 1/Mtb] ...
  (e.g., 1)= ? ');
K=input(' Number of Doppler grid points for calculation (e.g., 100) = ? ');
df=F/K/m_basic;

T=input(' Maximal Delay for ambiguity plot [in units of Mtb] (e.g., 1)= ? ');

N=input(' Number of delay grid points on each side (e.g. 100) = ? ');

sr=input(' Over sampling ratio (>=1) (e.g. 10)= ? ');

r=ceil(sr*(N+1)/T/m_basic);

if r==1
   dt=1;
   m=m_basic;
   uamp=abs(u_basic);
   phas=uamp*0;
   phas=angle(u_basic);
   if fcode==1
      phas=phas+2*pi*cumsum(f_basic);
   end
   uexp=exp(j*phas);
   u=uamp.*uexp;
else                              % i.e., several samples within a bit
   dt=1/r;                        % interval between samples
   ud=diag(u_basic);
   ao=ones(r,m_basic);
```

```
   m=m_basic*r;
   u_basic=reshape(ao*ud,1,m);    % u_basic with each element repeated r times
   uamp=abs(u_basic);
   phas=angle(u_basic);
   u=u_basic;
   if fcode==1
       ff=diag(f_basic);
       phas=2*pi*dt*cumsum(reshape(ao*ff,1,m))+phas;
       uexp=exp(j*phas);
       u=uamp.*uexp;
   end
end

t=[0:r*m_basic-1]/r;

tscale1=[0 0:r*m_basic-1 r*m_basic-1]/r;

dphas=[NaN diff(phas)]*r/2/pi;

% plot the signal parameters

figure(1), clf, hold off

subplot(3,1,1)
plot(tscale1,[0 abs(uamp) 0],'linewidth',1.5)
ylabel(' Amplitude ')
axis([-inf inf 0 1.2*max(abs(uamp))])

subplot(3,1,2)
plot(t, phas,'linewidth',1.5)
axis([-inf inf -inf inf])
ylabel(' Phase [rad] ')

subplot(3,1,3)
plot(t,dphas*ceil(max(t)),'linewidth',1.5)
axis([-inf inf -inf inf])
xlabel(' \itt / t_b ')
ylabel(' \itf * Mt_b ')

% calculate a delay vector with N+1 points that spans from zero delay to
%   ceil(T*t(m))
% notice that the delay vector does not have to be equally spaced but must
%   have all
% entries as integer multiples of dt
dtau=ceil(T*m)*dt/N;
tau=round([0:1:N]*dtau/dt)*dt;

% calculate K+1 equally spaced grid points of Doppler axis with df spacing
f=[0:1:K]*df;

% duplicate Doppler axis to show also negative Doppler's (0 Doppler is
%  calculated twice)
f=[-fliplr(f) f];

% calculate ambiguity function using sparse matrix manipulations (no loops)

% define a sparse matrix based on the signal samples u1 u2 u3 ... um
% with size m+ceil(T*m) by m (notice that u' is the conjugate transpose of u)
% where the top part is diagonal (u*) on the diagonal and the bottom part is a
%   zero matrix
```

```
%
%          [u1*  0   0  0 ...  0  ]
%          [ 0  u2*  0  0 ...  0  ]
%          [ 0   0  u3* 0 ...  0  ]  m rows
%          [ .             .   .  ]
%          [ .             .   .  ]
%          [ .   0   0  . ...   um*]
%          [ 0                  0 ]
%          [ .                  . ]   N rows
%          [ 0   0   0  0  ...  0 ]

mat1=spdiags(u',0,m+ceil(T*m),m);

% define a convolution sparse matrix based on the signal samples u1 u2 u3 ...
%   um
% where each row is a time(index) shifted versions of u.
% each row is shifted tau/dt places from the first row
% the minimal shift (first row) is zero
% the maximal shift (last row) is ceil(T*m) places
% the total number of rows is N+1
% number of columns is m+ceil(T*m)

% for example, when tau/dt=[0 2 3 5 6] and N=4
%
%          [u1 u2 u3 u4  ...               ... um  0  0  0  0  0  0]
%          [ 0  0 u1 u2 u3 u4  ...               ... um  0  0  0  0]
%          [ 0  0  0 u1 u2 u3 u4  ...               ... um  0  0  0]
%          [ 0  0  0  0  0 u1 u2 u3 u4  ...               ... um  0]
%          [ 0  0  0  0  0  0 u1 u2 u3 u4  ...               ... um]

% define a row vector with ceil(T*m)+m+ceil(T*m) places by padding u with zeros
% on both sides
u_padded=[zeros(1,ceil(T*m)),u,zeros(1,ceil(T*m))];

% define column indexing and row indexing vectors
cidx=[1:m+ceil(T*m)];
ridx=round(tau/dt)';

% define indexing matrix with Nused+1 rows and m+ceil(T*m) columns
% where each element is the index of the correct place in the padded version
%   of u
index = cidx(ones(N+1,1),:) + ridx(:,ones(1,m+ceil(T*m)));

% calculate matrix
mat2 = sparse(u_padded(index));

% calculate the ambiguity matrix for positive delays given by
%
%   [u1 u2 u3 u4  ...       ... um  0  0  0  0  0  0] [u1*  0   0  0 ...  0  ]
%   [ 0  0 u1 u2 u3 u4  ...       ... um  0  0  0  0] [ 0  u2*  0  0 ...  0  ]
%   [ 0  0  0 u1 u2 u3 u4  ...       ... um  0  0  0]*[ 0   0  u3* 0 ...  0  ]
%   [ 0  0  0  0  0 u1 u2 u3 u4  ...       ... um  0] [ .             .     .  ]
%   [ 0  0  0  0  0  0 u1 u2 u3 u4  ...       ... um] [ .             .     .  ]
%                                                    [ .   0   0  . ...  um*]
%                                                    [ 0                 0   ]
%                                                    [ .                 .   ]
%                                                    [ 0   0   0  0 ...  0  ]
%
% where there are m columns and N+1 rows and each element gives an element
% of multiplication between u and a time shifted version of u*. each row gives
```

```
% a different time shift of u* and each column gives a different entry in u.
%

uu_pos=mat2*mat1;
clear mat2 mat1

% calculate exponent matrix for full calculation of ambiguity function.
%   The exponent
% matrix is 2*(K+1) rows by m columns where each row represents a possible
%   Doppler and
% each column stands for a different place in u.

e=exp(-j*2*pi*f'*t);

% calculate ambiguity function for positive delays by calculating the integral
%   for each
% possible delay and Doppler over all entries in u.
% a_pos has 2*(K+1) rows (Doppler) and N+1 columns (Delay)
a_pos=abs(e*uu_pos');

% normalize ambiguity function to have a maximal value of 1
a_pos=a_pos/max(max(a_pos));

% use the symmetry properties of the ambiguity function to transform the
%   negative Doppler
% positive delay part to negative delay, positive Doppler
a=[flipud(conj(a_pos(1:K+1,:))) fliplr(a_pos(K+2:2*K+2,:))];

% define new delay and Doppler vectors
delay=[-fliplr(tau) tau];
freq=f(K+2:2*K+2)*ceil(max(t));

% excludes the zero Delay that was taken twice
delay=[delay(1:N) delay(N+2:2*N)];
a=a(:,[1:N,N+2:2*N]);

% plot the ambiguity function and autocorrelation cut
[amf amt]=size(a);

% create an all blue color map
cm=zeros(64,3);
cm(:,3)=ones(64,1);

figure(2), clf, hold off
mesh(delay, [0 freq], [zeros(1,amt);a])

hold on
surface(delay, [0 0], [zeros(1,amt);a(1,:)])

colormap(cm)
view(-40,50)
axis([-inf inf -inf inf 0 1])
xlabel(' {\it\tau}/{\itt_b}','Fontsize',12);
ylabel(' {\it\nu}*{\itMt_b}','Fontsize',12);
zlabel(' |{\it\chi}({\it\tau},{\it\nu})| ','Fontsize',12);
hold off
```

PROBLEMS

3.1 Ambiguity function of a time-scaled signal
If the ambiguity function of $u(t)$ is $|\chi(\tau, \nu)|$, prove that the ambiguity function $|\chi_1(\tau, \nu)|$ of $u_1(t) = u(at)$ is given by

$$|\chi_1(\tau, \nu)| = \frac{1}{a}\left|\chi\left(a\tau, \frac{\nu}{a}\right)\right|$$

3.2 Calculation of the AF using a signal's Fourier transform
Prove that the ambiguity function can also be written in the form

$$|\chi(\tau, \nu)| = \left|\int_{-\infty}^{\infty} U^*(f)U(f - \nu)\exp(j2\pi f\tau)\, df\right|$$

where $U(f)$ is the Fourier transform of $u(t)$.

3.3 Doppler resolution connection to signal amplitude
Show that for a normalized signal ($E = 1$),

$$\frac{\partial^2\chi(0, 0)}{\partial\nu^2} = -4\pi^2\int_{-\infty}^{\infty} t^2|u(t)|^2\, dt$$

3.4 Prove equation (3.39).

3.5 Another form of the ambiguity function
In the ambiguity function (3.1), change the integration variable t to t_1 by using

$$t = t_1 - \frac{\tau}{2}$$

and obtain another form of the ambiguity function.

REFERENCES

Freedman, A., and N. Levanon, Properties of the periodic ambiguity function, *IEEE Transactions on Aerospace and Electronic Systems*, vol. 30, no. 3, May 1994, pp. 938–941.

Getz, B., and N. Levanon, Weight effects on the periodic ambiguity function, *IEEE Transactions on Aerospace and Electronic Systems*, vol. 31, no. 1, January 1995, pp. 182–193.

Mozeson, E., and N. Levanon, MATLAB code for plotting ambiguity functions, *IEEE Transactions on Aerospace and Electronic Systems*, vol. 38, no. 3, July 2002, pp. 1064–1068.

Papoulis, A., *Signal Analysis*, McGraw-Hill, New York, 1977, Chap. 8.

Rihaczek, A. W., *Principles of High Resolution Radar*, McGraw-Hill, New York, 1969.